

Accurate determination of the low-angle structure factors of β NiAl by powder X-ray diffraction

Alan G. Fox^{a,*}, E. Sarath K. Menon^b

^a Faculty of Engineering and Technology, Asian University, 89 Moo 12, Highway 331, Banglamung, Chon Buri 20150 Thailand

^b Centre for Materials Science and Engineering, Department of Mechanical and Astronautical Engineering, Naval Postgraduate School, Monterey, CA 93943, USA

*Corresponding author, e-mail: afox@asianust.ac.th

Received 3 Nov 2011

Accepted 11 Apr 2012

ABSTRACT: An improved approach to the analysis of powder X-ray diffractometer data obtained from crystalline materials has been developed and applied to diffraction data obtained from powdered β Ni-50.51 at% Al (B2 cubic structure) with Cu-K α radiation. Great care was taken to ensure the accuracy of the alloy chemical analysis and very fine powders (less than 5 μ m particle size) were used to minimize the effects of preferred orientation and extinction. As a result it was found that, even when only a few reflections are available for study and anomalous dispersion corrections and thus extinction corrections are somewhat larger than normal due to excessive fluorescence, it is possible to obtain accurate low-angle structure factor values that give information about crystal bonding. In the case of β NiAl, this appears to be predominantly ionic. These results mean that any laboratory that has a basic powder X-ray diffractometer can adopt this approach and make accurate measurements of the structure factors of many crystalline solids.

KEYWORDS: Debye-Waller factors, extinction and dispersion corrections, charge density

INTRODUCTION

Accurate measurements of the structure factor amplitudes and the Debye-Waller factors of elements and binary systems by electron, X-ray and gamma-ray diffraction have made important contributions to the understanding of the nature of bonding in these materials (see, for example, Fox¹ for a review, and also some later journal articles²⁻⁵). In principle, X-ray and γ -ray diffraction should be the most effective methods to determine the structure factor amplitudes of crystals. Unfortunately, corrections due to anomalous dispersion, extinction, and preferred orientation (for powder samples) can make such measurements difficult to perform with sufficient accuracy to investigate the effects of bonding in materials. In addition, for metallic alloys, the composition must be very accurately known and the heat treatment before and after powdering must be carefully performed. Despite these difficulties, X-ray diffraction experiments have proved somewhat successful in determining the contributions to the bonding charge density from low-angle structure factors because the effects of extinction and preferred orientation can be minimized by the use of very fine (< 5 μ m particle size) powders^{6,7}. For single crystal samples, extinction is inevitable, even with high energy gamma radiation^{8,9}

and its effects are strongest at low angles. Extinction makes it difficult to measure low-angle structure factors with sufficient accuracy to investigate the charge densities of materials and, so, many single crystal studies have focused on the measurement of higher angle structure factors, with a view to the accurate measurement of atom positions and Debye-Waller factors^{10,11}. Convergent beam (CBED) and Kikuchi electron diffraction methods have proved extremely effective for the measurement of the lowest angle structure factors^{1,4,5} but unfortunately it is difficult to determine Debye-Waller factors by this technique except for relatively simple structures. These difficulties have led to combinative techniques where X-ray diffraction measurements of structure factors are 'normalized' by the use of low-angle electron diffraction measurements^{12,13}. This approach has proved very successful at providing information about the charge densities of several materials. In addition to these experimental measurements of structure factors, recent first principles calculations have proved to be very effective for determining electron charge density distributions and thus the crystal structure factors of elements and binary alloys^{4,5,14,15}. In this work, it will be demonstrated that careful powder diffraction measurements made on β NiAl are fully capable of making accurate determinations of low-

angle structure factors that agree very closely with those determined by first principles calculations and electron diffraction experiments. These indicate that bonding in β NiAl is mostly ionic.

MATERIALS AND METHODS

Sample chemistry

Structure factor data for β NiAl from the following sources was assessed—Fox and Tabbernor^{16,17} (electron diffraction), Cooper^{18,19} (X-ray powder diffraction) and Georgopoulos and Cohen¹⁰ (single crystal X-ray diffraction—high accuracy Debye-Waller factor measurements only). More recently Sang, Kulovits and Wiezorek²⁰ have made accurate electron diffraction measurements of three lower order structure factors in β NiAl (the (100), (110), and (200)) and these are in excellent agreement with those of Fox¹⁷. Each of these authors claimed to have examined a stoichiometric alloy (50 at.%) with Cooper^{18,19} and Georgopoulos and Cohen¹⁰ examining some off-stoichiometric alloys as well. Unfortunately, it has proved difficult to determine the exact chemical compositions of intermetallic aluminides (especially γ TiAl) accurately by measuring losses on melting or by conventional chemical analysis methods¹⁸, although a standardised X-ray fluorescence spectrometer or wavelength dispersive X-ray spectroscopy in an electron probe/SEM can be very effective. In the present work great care was taken to accurately determine the alloy chemistry by all these techniques and the best value was found to be Ni-50.51 at.% Al with a standard error of 0.05 at.%. To examine the structure factors and charge density of a binary alloy it is also essential to have an accurate knowledge of the lattice parameter(s) of the sample under consideration. This has also proved difficult for β NiAl because it would seem that, as soon as an alloy is analysed as being aluminium-rich, both Al antistructure atoms and constitutional vacancies can exist when the composition exceeds about 50.7 at.% Al. It would therefore seem that the sample studied in the present work did not contain constitutional vacancies. Numerous lattice parameter measurements have been made on β NiAl with chemistries near stoichiometry², but these analyses have been complicated by the fact that powdered β NiAl apparently oxidizes when annealed in 'vacuum'²¹. In addition, lattice parameters can be affected by strains developed during the powdering of samples. There can be microstresses leading to line broadening and/or macrostresses that are likely to be compressive. The latter lead to overall mean strains and thus effective reductions in lattice parameters.

For example, the data of Cooper¹⁸ indicate that his samples were not annealed after powdering.

Sample Preparation

After melting and homogenizing at 1573 K for three days, the samples from all sources were powdered and sieved for X-ray diffraction. The sample of Cooper¹⁸ was passed through a 400 mesh (37 μ m) sieve, ground further to reduce the particle size and then pressed into a die using a compacting pressure of 276 MPa. It should be mentioned that such a procedure is highly likely to produce preferred orientation although Cooper claimed that this was minimal. The sample of the present work was powdered and sieved through conventional 350 and 400 mesh sieves and then through an acoustic sieve with electrically formed metallic screens of 20, 10 and finally 5 μ m spacing as described by Parrish and Hart⁷. After sieving, the powders were annealed at 973 K for 1 h in pure argon. This procedure ensured that only secondary extinction was present in the final sample (< 5 μ m particle size). Samples for X-ray diffraction were obtained at each stage of sieving but only those in the particle size ranges 45–38 μ m and < 5 μ m were studied in the present work. To avoid preferred orientation, the samples were mounted in a Philips powder X-ray diffractometer holder using hand pressure only and the sample was held together with a solvent based binder. This procedure ensured minimal preferred orientation, surface roughness and inhomogeneity in the sample. An examination of the backgrounds of all the samples studied together with the background obtained from a polished and etched polycrystalline sample showed these to be all very similar suggesting that sample oxidation was not a problem in this work.

Data analysis

X-ray diffractograms were collected from the elevated Bragg reflections of the β NiAl sample described above at 293 K using a Philips PW1710 diffractometer operated at 30 kV and 30 mA with a Cu target and a bent graphite crystal monochromator. Nelson-Riley analyses of the peak intensities produced lattice parameter values for the two samples studied. Attempts were made to evaluate the experimental intensities using proprietary versions of the Rietveld procedure. Unfortunately, because of the large background present due to the fluorescence of Ni by the Cu-K α radiation, the computer programs returned errors which stated that functional modelling of the diffracted intensities was not possible. It is well known that problems can arise with the mathematical modelling of X-ray reflections to provide intensity

input for a Rietveld analysis⁷ and so we reverted to the use of conventional planimetry to obtain the experimental intensity data needed. This proved to be highly effective and reproducible particularly because there is no overlap between reflections with different (hkl) for β NiAl with Cu-K $_{\alpha}$ radiation.

The theoretical intensities of Al-rich β NiAl alloys (B2 cubic) that do not contain constitutional vacancies can be calculated from the following fundamental and superlattice structure factors, respectively.

$$F_{hkl} = 2m_{\text{Ni}}f_{\text{Ni}} e^{-M_{\text{Ni}}} + 2m_{\text{Al}}f_{\text{Al}} e^{-M_{\text{Al}}} \quad (1a)$$

$$F_{hkl} = 2m_{\text{Ni}}(f_{\text{Ni}} e^{-M_{\text{Ni}}} - f_{\text{Al}} e^{-M_{\text{Al}}}) \quad (1b)$$

The $m_{\text{Ni(Al)}}$ are the atom fractions of nickel (aluminium); the $M_{\text{Ni(Al)}}$ are the temperature corrections for the Ni (Al) atoms which include a correction for thermal diffuse scattering (these are small for β NiAl at 293 K because of its high melting point). These are given by:

$$M_{\text{Ni(Al)}} = B_{\text{Ni(Al)}} \sin^2 \theta / \lambda^2, \quad (2)$$

where the $B_{\text{Ni(Al)}}$ are the Debye-Waller factors at the temperature of measurement including the contributions of thermal diffuse scattering. In the case of stoichiometric β NiAl, $B_{\text{Ni}} \approx B_{\text{Al}}$ (see Table 1) and so the determination of an average Debye-Waller factor (B_{avg}) is a useful exercise. For the analysis of the electron diffraction data, the $f_{\text{Ni(Al)}}$ are the atomic scattering factors of the Ni(Al) atoms for electrons. These can be converted to (and from) the atomic scattering factors for X-rays (without dispersion corrections) by the usual Mott formula²³. For X-ray analyses, the f values include the dispersion corrections $\Delta f'$ and $\Delta f''$ so that

$$f_{\text{Ni(Al)}} = f_{0(\text{Ni(Al)})} + \Delta f'_{\text{Ni(Al)}} + i\Delta f''_{\text{Ni(Al)}}. \quad (3)$$

The theoretical (calculated) X-ray integrated intensities for reflections (hkl), I_{hkl} can now be expressed using the usual equation

$$I_{hkl} = KP_{hkl}\phi|F_{hkl}|^2E_{hkl}, \quad (4)$$

where K is the scaling factor, P_{hkl} is the multiplicity factor, ϕ is the Lorentz-Polarization correction and E_{hkl} is the extinction correction which was calculated using the theory of Sabine²⁴. The F_{hkl} were calculated using free atom values of the atomic scattering factors and dispersion corrections from²². Values of K , B_{Ni} and B_{Al} (or B_{avg}), and the coherent region average diameter, d , were then found that led to a minimum in the R factor given by

$$R = \sum_{i=1}^N (I_i^{\text{observed}} - I_i^{\text{calculated}})^2 / I_i^{\text{observed}}. \quad (5)$$

The $I_i^{\text{calculated}}$ were evaluated using equations (1) to (4) and the I_i^{observed} is the measured intensity for reflection (hkl). This procedure assumes Poisson statistics and $R = 1.0$ for a perfect fit²⁵. Once the values of K , B_{Ni} and B_{Al} (or B_{avg}), and d are found the data can be analysed to produce best values of F_{hkl} and then the static structure factors, $F_0(hkl)$, which incorporate no temperature or dispersion corrections can be calculated. The analysis of critical voltage CBED/Kikuchi electron diffraction data to measure $F_0(hkl)$ have been described in detail^{16,17}. These results are shown in Table 1. High quality first principles calculations of the low-angle structure factors of equiatomic (stoichiometric) β NiAl have been made by Lu et al¹⁴ and these were used for comparison with the experimental data assessed in the present work and are also shown in Table 1.

RESULTS

The intensity data of Cooper¹⁹ were obtained using Ag-K $_{\alpha}$ radiation ($\lambda_{\text{average}} = 0.561 \text{ \AA}$) and analysed assuming an equiatomic composition with appropriate dispersion corrections and lattice parameter $a = 2.8864 \text{ \AA}$. Cooper established an absolute scale for his data and assumed the absence of extinction and preferred orientation. The absolute scale was referred to the β NiAl (110) reflection and had an estimated error of 1.3%; the value of B_{avg} obtained in this way was 0.37 \AA^2 . Despite Cooper's assertion that preferred orientation was absent from his data, there is clear evidence for the reduction of the ($h00$) intensities due to this. In this work we rescaled Cooper's data using the method outlined below (using the free atom values of the structure factors $F_0(hkl)$) and we did not include the (100) and (200) reflections in the analysis. In addition, like Cooper, we also ignored the effects of extinction. This calculation produced a value of $B_{\text{avg}} = 0.35 \pm 0.03 \text{ \AA}^2$ and a value of $R = 8.07$. This value of R is rather high but is improved to 3.74 using first principles values of $F_0(hkl)$. Despite this, the value of B_{avg} agrees well with that obtained by Cooper (0.37 \AA^2). A set of experimental values of $F_0(hkl)$ with associated errors were calculated and these are shown in Table 1. It should be pointed out that the values of B_{avg} and $F_0(hkl)$ determined in this way by scaling the intensities to free atom values of $F_0(hkl)$ can be approximate because of bonding effects (see Menon and Fox³ on γ -TiAl for an example). In the case of β NiAl it will be seen that this procedure does not lead to inaccurate values of B_{avg} and $F_0(hkl)$ because the effects of bonding are relatively small. The two sets of intensity data acquired in the present work were obtained with Cu-K $_{\alpha}$ radiation ($\lambda_{\text{average}} =$

Table 1 Experimental and theoretical static structure factors, $F_0(hkl)$, of βNiAl .

| (hkl) | Composition 50 at.% Al (previous work) | | | | Composition 50.5 at.% Al (present work) | | | |
|-------------------------------------|--|------------------------------------|--------------------------------|------------------------------|--|--|--------------------------------|------------------------------|
| | Calculated from Ref. 19 | Electron diffraction ¹⁷ | Theory free atom ²² | Theory crystal ¹⁴ | 38–45 μm powder particle size | < 5 μm powder particle size | Theory free atom ²² | Theory crystal ¹⁴ |
| 100 | 12.91 \pm 0.08 | 13.67 \pm 0.05 | 13.52 | 13.67 | 13.44 \pm 0.07 | 13.48 \pm 0.07 | 13.37 | 13.52 |
| 110 | 29.01 | 28.92 \pm 0.10 | 29.14 | 28.91 | 28.72 \pm 0.15 | 28.90 \pm 0.15 | 29.02 | 28.88 |
| 111 | 10.84 \pm 0.14 | 10.76 \pm 0.22 | 10.85 | 10.74 | 10.70 \pm 0.08 | 10.74 \pm 0.08 | 10.74 | 10.63 |
| 200 | 23.35 \pm 0.23 | 24.41 \pm 0.12 | 24.57 | 24.40 | 24.29 \pm 0.15 | 24.36 \pm 0.15 | 24.47 | 24.30 |
| 210 | 8.97 \pm 0.11 | | 9.06 | 8.97 | 8.94 \pm 0.08 | 8.94 \pm 0.08 | 8.97 | 8.88 |
| 211 | 21.36 \pm 0.16 | | 21.4 | 21.32 | 20.83 \pm 0.15 | 21.13 \pm 0.15 | 21.32 | 21.24 |
| 220 | 18.62 \pm 0.25 | | 19.01 | 18.96 | 19.17 \pm 0.16 | 19.08 \pm 0.16 | 18.94 | 18.89 |
| 300/221 | 7.24 \pm 0.11 | | 7.02 | 7.02/7.03 | 7.00 \pm 0.08 | 6.95 \pm 0.08 | 6.95 | 6.95 |
| 310 | 16.91 \pm 0.26 | | 17.14 | 16.93 | 17.26 \pm 0.15 | 17.16 \pm 0.15 | 17.07 | 16.86 |
| 311 | Not reported | | 6.43 | 6.45 | 6.25 \pm 0.08 | 6.36 \pm 0.08 | 6.37 | 6.39 |
| 222 | 15.62 \pm 0.28 | | 15.64 | 15.62 | 15.26 \pm 0.16 | 15.31 \pm 0.16 | 15.28 | 15.27 |
| B_{avg} (\AA^2) | 0.35 \pm 0.03 | 0.49 \pm 0.02 | | | 0.52 \pm 0.04 | 0.49 \pm 0.02 | | |
| B_{Ni} (\AA^2) | | 0.51 ¹⁰ | | | | 0.51 \pm 0.03 | | |
| B_{Al} (\AA^2) | | 0.47 ¹⁰ | | | | 0.48 \pm 0.03 | | |
| R (free atom) | 8.07 | | | | 5.93 | 1.58 | | |
| R (crystal) | 3.74 | | | | 5.76 | 1.31 | | |
| d (μm) | | | | | 1.25 | 0.58 | | |

(hkl) are the Miller indices, B_{avg} is the average Debye-Waller factor, $B_{\text{Ni(Al)}}$ are the Debye-Waller factors for Ni(Al) atoms, respectively, R is the least squares goodness of fit parameter, and d is the coherent region diameter as discussed in the text.

1.542 \AA) and analysed using a composition of Ni-50.51 at.% Al (best chemical analysis) with

$$\begin{aligned} \Delta f'_{\text{Ni}} &= -3.0029, & \Delta f''_{\text{Ni}} &= 0.5091, \\ \Delta f'_{\text{Al}} &= 0.2130, & \Delta f''_{\text{Al}} &= 0.2455, \end{aligned}$$

obtained from Creagh and McAuley²⁶ and $a = 2.88806 \text{ \AA}$ (calculated from a Nelson-Riley fit to the peaks of the intensity data acquired from the sample with powder particle size less than 5 μm). The intensity data for both samples were then analysed as discussed previously and extinction was taken into account using the method of Sabine²⁴ from which values of the coherent region sizes (diameters), d , were calculated; these are shown in Table 1. In the present work, preferred orientation may have been present but it appears to be minimal and was thus ignored. Values of B_{avg} and R were obtained from the analyses and these are also shown in Table 1, together with sets of calculated values of $F_0(hkl)$ and associated errors.

DISCUSSION

The values of $F_0(hkl)$ derived from the data of Cooper¹⁹ are good enough to deduce that the structure of βNiAl is B2 and that is all. They are not nearly good enough to distinguish between the free atom structure factors and the first principles calculations as shown in Table 1 even if the more likely composition of 50.7 at.% is adopted in the analysis. This is not surprising as preferred orientation was certainly present in Cooper's sample and there is the likelihood

of extinction as well, since the value of B_{avg} obtained from Cooper's data was $0.35 \pm 0.03 \text{ \AA}^2$ which is lower than the accepted value of $B_{\text{avg}} = 0.49 \text{ \AA}^2$ ¹⁷. As discussed previously, the ignoring of extinction leads to a reduction in B_{avg} to 0.35 \AA^2 and the values of R (8.07 and 3.74) suggest that the reflection set that excludes (100) and (200) contain useful bonding information if the data could be rescaled with the correct Debye-Waller factor. The results obtained from the intensity data in the present work give much greater cause for optimism in that it would seem that powder X-ray diffraction can be used to extract low-angle bonding information for βNiAl . The sample with the powder size range 37 μm to 45 μm gives $R = 5.93$ ($F_0(hkl) = \text{free atom}$), $B_{\text{avg}} = 0.52 \pm 0.04 \text{ \AA}^2$ and a coherent region diameter of 1.25. The latter is much smaller than the powder particle size and reflects an average sub-grain size (diameter) associated with powdering and annealing. The experimental values of the static structure factors, $F_0(hkl)$, have significant errors but are for the most part reflecting the bonding trend in βNiAl and the experimental value of B_{avg} is in good agreement with the value of Fox¹⁷ obtained by electron diffraction as shown in Table 1. It should be noted that the experimental structure factors are closer on average to the first principle calculation of $F_0(hkl)$ rather than the free atom values as the value of R is reduced to 5.76 when these are used for the intensity analysis. For the sample with the powder particle size range < 5 μm analysis gives $R = 1.58$ ($F_0(hkl) = \text{free atom}$), $B_{\text{avg}} = 0.49 \pm 0.02 \text{ \AA}^2$, and $d = 0.58 \mu\text{m}$ and now the agreement between the experimental

values of $F_0(hkl)$ and first principles calculations is excellent (Table 1). When a comparison is made with free atom values, the experimental static structure factors are found to be slightly different to their free atom counterparts but in agreement with them within experimental error; this is also evident from Table 1. In Fig. 1, a Wilson plot of these data is presented and this suggests that the greatest errors are associated with the (220) and (310) reflections and this is also confirmed by the data in Table 1. Fig. 2 illustrates that the agreement between the calculated intensities obtained using free atom values of $F_0(hkl)$ and the experimental intensities is improved by determining the two individual Debye-Waller factors B_{Ni} and B_{Al} to obtain R instead of the single value, B_{avg} . This procedure, however, does not reduce R from its Wilson plot value of 1.58. However, the use of the first principles calculated values of $F_0(hkl)$ and B_{avg} in the analysis gives $R = 1.31$, a significant improvement that confirms the suggestion that bonding in $\beta NiAl$ is predominantly ionic. Despite this excellent agreement between experiment and theory, the estimated errors in the experimental values of $F_0(hkl)$ at the lowest angles are such that the accuracy appears to be only just sufficient for bonding charge density studies. However, a large component of these errors arises from the (perhaps over-pessimistic) assessment of the uncertainties in the values of the anomalous dispersion corrections for nickel in $\beta NiAl$ which are rather large for Cu- K_{α} radiation. The use of Mo- K_{α} radiation ($\lambda_{average} = 0.711 \text{ \AA}$) would give much smaller values of the dispersion corrections and provide more reflections for analysis. This would perhaps allow for more accurate measurement of the Debye-Waller and structure factors. Alternatively, (preferably) the experiment could be performed with appropriately tuned synchrotron radiation if one is available. It should also be mentioned that the low-angle measurements made by powder X-ray diffraction (taking into account the 0.5 at.% difference in composition) agree very closely with those determined by electron diffraction. This is also shown in Table 1. Finally, the method adopted for powder X-ray diffraction in the present work is recommended to all workers performing routine powder diffraction measurements on crystalline materials since it will give improved accuracy for all experiments of this type.

Acknowledgements: The authors would like to thank the President of Asian University, Dr Viphandh Roengpithya and Superintendent's Office of the Naval Postgraduate School for provision of financial support and laboratory and computing facilities. Financial support from the Materi-

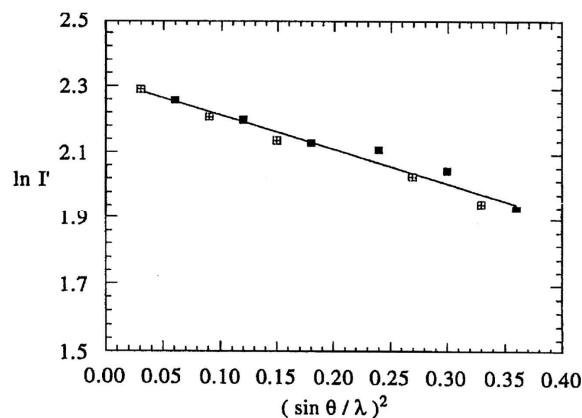


Fig. 1 Wilson Plot of the X-ray intensities obtained from powdered $\beta NiAl$ with a maximum particle size of 5 μm . The solid squares refer to the fundamental reflections and the open and crossed squares to the superlattice reflections. The least-squares fit line is shown.

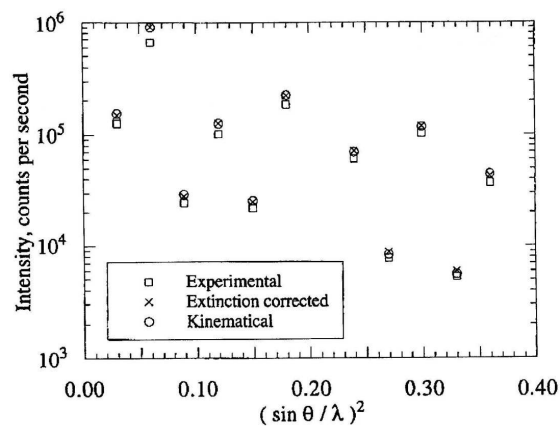


Fig. 2 Plot demonstrating the procedure adopted to compute the individual Debye-Waller factors, B_{Ni} and B_{Al} in the powdered $\beta NiAl$ sample with a particle size of less than 5 μm . The experimental data (open squares) were corrected for extinction to produce the set of intensities shown by crosses. The kinematical theory values (open circles) were calculated from equations (1) to (4) using free atom values of the atomic scattering factors. The agreement between extinction corrected data and kinematical theory is clearly very good when the least squares fit routine (5) is applied to the data to produce the best values of the B_{Ni} and B_{Al} and the R factor of 1.58 shown in Table 1.

als Directorate, Wright-Patterson Air Force Base, Dayton, Ohio 45433, USA under contract no. FY1457-94-N5026 (Monitor, Dr D. Dimiduk) and the Aircraft Division, Naval Air Development Centre, Warminster, Pennsylvania 18974,

USA under contract no. N62269-94-WR-00217 (Monitor, Dr J. Waldman) is also gratefully acknowledged.

REFERENCES

1. Fox AG (1993) Is it feasible to determine the bonding charge density of stoichiometric γ TiAl through structure factor measurements? *Phil Mag Lett* **68**, 29–37.
2. Fox AG, Menon ESK (1997) Structure factors and bonding in β NiAl. *J Phase Equil* **18**, 509–15.
3. Menon ESK, Fox AG (1998) Debye-Waller factors of stoichiometric and Al-rich γ -TiAl alloys. *Phil Mag A* **77**, 577–92.
4. Saunders M, Fox AG, Midgley PA (1999) Structure factor measurement by ZAPMATCH. *Acta Crystallogr A* **A55**, 471–9.
5. Saunders M, Fox AG, Midgley PA (1999) Debye-Waller factor measurement by ZAPMATCH. *Acta Crystallogr A* **A55**, 480–8.
6. Rantavuori E, Tanninen VP (1977) The atomic scattering factors of powdered aluminium at 80 K. *Phys Scr* **15**, 273–5.
7. Parrish W, Hart M (1988) Accurate measurement of powder diffraction intensities using synchrotron radiation. *Aust J Phys* **41**, 403–11.
8. Schneider JR, Hansen NK, Kretschmer H (1981) A charge density study of copper by γ -ray diffraction on imperfect single crystals. *Acta Crystallogr A* **A37**, 711–22.
9. Mackenzie JK, Mathieson AMcL (1992) Band structure calculations and structure factor estimates of Cu—their complementarity. *Acta Crystallogr A* **A48**, 231–6.
10. Georgopoulos P, Cohen JB (1977) The defect structure and Debye-Waller factors versus composition in β Ni_{1±x}Al_{1±x}. *Scripta Metall* **11**, 147–50.
11. Swaminathan S, Jones IP, Maher DM, Johnson AW, Fraser HL (1996) Debye-Waller factors in off-stoichiometric TiAl: effect of ordering of excess Al atoms on Ti sites. *Phil Mag Lett* **73**, 319–30.
12. Fox AG, Tabernor MA, Fisher RM (1990) Low-angle atomic scattering factors and charge density of aluminum. *J Phys Chem Solid* **51**, 1323–8.
13. Zuo JM, Kim M, O'Keefe M, Spence JCH (1999) Direct observation of d holes and Cu-Cu bonding in Cu₂O. *Nature* **401**, 49–52.
14. Lu ZW, Wei S-H, Zunger A (1992) Theory of bonding charge density in β NiAl. *Acta Metall Mater* **40**, 2155–65.
15. Lu ZW, Zunger A, Fox AG (1994) Comparison of experimental and theoretical electronic charge distributions in γ TiAl. *Acta Metall Mater* **42**, 3929–43.
16. Fox AG, Tabernor MA (1991) The bonding charge density of β NiAl. *Acta Metall Mater* **39**, 669–78.
17. Fox AG (1995) Low-angle structure factors, Debye temperatures and charge density of NiAl: A reconciliation between experiment and first principles full potential linear augmented plane wave (FLAPW) calculations in the local density approximation. *Scripta Metall* **32**, 343–7.
18. Cooper MJ (1963) An investigation of the ordering of the phases CoAl and NiAl. *Phil Mag* **8**, 805–10.
19. Cooper MJ (1963) The electron distribution in the phases CoAl and NiAl. *Phil Mag* **8**, 811–21.
20. Sang XH, Kulovits A, Wiezorek JMK (2011) Simultaneous determination of highly precise Debye-Waller factors and structure factors for chemically ordered NiAl. *Acta Crystallogr* **A66**, 694–702.
21. Fraser HL, Loretto MH, Smallman RE, Wasilewski RJ (1973) Oxidation induced defects in NiAl. *Phil Mag* **28**, 639–50.
22. Maslen EN, Fox AG, O'Keefe MA (1992) X-ray scattering. Wilson AJC (ed) *International Tables for Crystallography* Vol. C, Kluwer, Dordrecht, Section 6.1.1, pp 476–511 and 533–4.
23. Mott NF, Massey HSW (1965) *The Theory of Atomic Collisions*, 3rd edn, Oxford Univ Press, Oxford UK.
24. Sabine TM (1988) A reconciliation of extinction theories. *Acta Crystallogr* **A44**, 368–74.
25. Prince E, Spiegelmann CH (1992) The χ^2 distribution. Wilson AJC (ed) *International Tables for Crystallography* Vol. C, Kluwer, Dordrecht, Section 8.4.1, pp 618–9.
26. Creagh DC, McAuley WJ (1992) X-ray dispersion corrections. Wilson AJC (ed) *International Tables for Crystallography* Vol. C, Kluwer, Dordrecht, Section 4.2.6, pp 206–22.